Dynamics and Control of Integrated Networks with Purge Streams

Michael Baldea and Prodromos Daoutidis
Dept. of Chemical Engineering and Materials Science, University of Minnesota, Minneapolis, MN 55455

Aditya Kumar
GE Global Research, Schenectady, NY 12301

DOI 10.1002/aic.10756
Published online January 12, 2006 in Wiley InterScience (www.interscience.wiley.com).

This work concerns the dynamics and control of process networks in which impurities are present and are removed by a small purge stream. Using a singular perturbation analysis, it is shown that the presence of the small purge stream leads to a time scale separation in the dynamics of the network. A method is proposed for the derivation of nonstiff, reduced-order models in each time scale that are suitable for analysis and model-based control. Finally, two case studies are introduced and illustrative numerical simulation results are provided. © 2006 American Institute of Chemical Engineers *AIChE J,* 52: 1460–1472, 2006

Keywords: process networks, model reduction, purge, nonlinear control

Introduction

Process networks, consisting of reaction and separation units interconnected through material and energy recycle streams, represent the rule rather than the exception in the process industries. The dynamics and control of such networks present distinct challenges, given that, in addition to the nonlinear behavior of the individual units, the feedback interactions among these units, induced by recycle, typically give rise to more complex overall network dynamics.[1,2] Design modifications (such as adding surge tanks between different units to attenuate disturbances propagating through the recycle) can in principle be used to minimize these interactions, although such modifications are not favored by the recent demands for lower capital and operating costs, and tighter process integration.

At the same time, the efficient *transient* operation of such networks is becoming increasingly important, as the current environment of frequent changes in market conditions and economic objectives dictates frequent changes in operating conditions and targets (such as product grade transitions, feed switching, and so on) and tighter coordination of the plantwide optimization and advanced control levels.[3] A major bottleneck toward analyzing, optimizing, and better controlling the dynamics of such networks is the often overwhelming size and complexity of their dynamic models, which make dynamic simulation computationally intensive, and the design of fully centralized nonlinear controllers on the basis of entire network models impractical—such controllers are almost invariably difficult to tune, expensive to implement and maintain, and sensitive to modeling errors and measurement noise. Indeed, the majority of studies on control of networks with recycle (see, for example, Yi and Luyben,[4] Chen and Yu,[5] and Skogestad[6]) are within a multiloop linear control framework. In a different vein, a formal framework for stability analysis and stabilization of process networks, based on passivity and concepts from thermodynamics, was recently postulated in Hangos et al.[7] and Ydstie.[8] Thus, the development of a systematic framework for analyzing the nonlinear dynamic interactions induced by recycle structures, and rationally accounting for them in the controller design, clearly remains an important open problem.

In our previous work,[9] we considered process networks with large material recycle compared to the throughput. Within the

Correspondence concerning this article should be addressed to P. Daoutidis at this current address: Aristotle University of Thessaloniki, Thessaloniki, Greece; e-mail: daoutidi@cems.umn.edu.

framework of singular perturbations, we established that the large recycle induces a time scale separation, with the dynamics of individual processes evolving in a fast time scale with weak interactions, and the dynamics of the overall system evolving in a slow time scale where these interactions become significant; this slow dynamics is usually nonlinear and of low order. Motivated by this, we proposed: (1) a model reduction method for deriving nonlinear low-order models of the slow dynamics induced by large recycle streams and (2) a controller design framework consisting of properly coordinated controllers in both the fast and the slow time scales.

In this report we focus on process networks with a recycle stream and a purge stream. The latter is typically used for the removal of impurities (introduced as part of the feed streams and/or reaction byproducts); the presence of the recycle can lead to the accumulation of such impurities in the recycle loop, which can in turn be detrimental to the process operation (for example, by poisoning the catalyst in the reactor) and the process economics.[10-12] Understanding the dynamics of the impurities is thus critical and controlling the level of such components in the recycle structure can be a key operational objective.

In almost all such networks with purge streams, the magnitude of these streams is significantly smaller than that of the throughput and/or the recycle streams, so that raw materials losses and/or pollution can be minimized. This suggests the possibility of a "core" dynamics over a much slower time scale compared to the dynamics of the individual process units and possibly the overall network dynamics. Developing an explicit nonlinear model of this slow dynamics can be beneficial both for analysis and evaluation purposes, and for model-based control.

In what follows, we begin by introducing two motivating examples of process networks with recycle and purge. First, we analyze the case of a reactor with gas effluent connected by a gas recycle stream to a condenser, and a purge stream used to remove the light inert components. In the second case, the products of a liquid-phase reactor are separated by a distillation column. The bottoms of the column are recycled to the reactor, and the heavy inert that is present in the feed stream is removed by a liquid purge stream. We show that, in both cases, the dynamics of the network is modeled by a system of stiff ordinary differential equations (ODEs) that can, potentially, exhibit a two-time scale behavior.

Motivated by the above, we consider a generic process network structure consisting of a reaction–separation sequence in which impurities are present and a purge stream is used for their removal. We show that in the general case, the dynamics of such networks is described by a system of ODEs in a nonstandard singularly perturbed form. We investigate the dynamic behavior of the class of process networks considered within the framework of singular perturbations, demonstrating that indeed they exhibit a two-time scale dynamics and deriving explicit reduced-order, nonstiff models for the dynamics in each time scale. We also establish that the slow dynamics of the networks considered is one-dimensional and is associated with the total inert holdup in the recycle loop, which represents a true slow variable of the network. Also, we highlight the control implications of the two-time scale dynamics of these systems, that is, the separation of the available flow rates into two groups of manipulated inputs that act on and can be used for addressing control objectives in the two time scales. Finally, we provide numerical simulations illustrating the theoretical concepts developed.

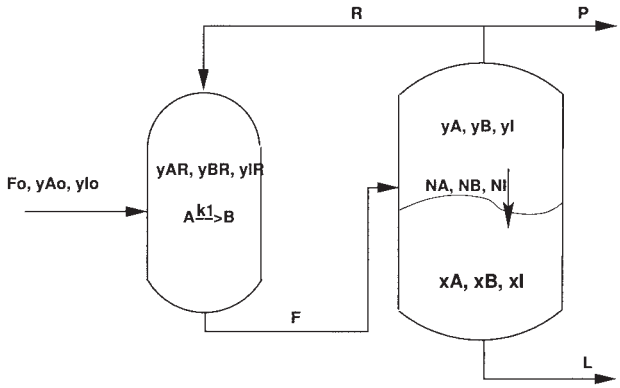

Figure 1. Process network with recycle and purge.

Motivating Examples I

Process networks with recycle and light inerts

Consider the network of a gas-phase reactor and a condenser shown in Figure 1. The reactant A is fed at a molar flow rate F_o to the reactor, where a first-order irreversible reaction $A \rightarrow B$ takes place with a reaction rate constant k_1. The outlet stream from the reactor is fed to a partial condenser that separates the light unconverted reactant A from the heavy product B. The gas phase, rich in A, is recycled back to the reactor. It is also assumed that a very volatile inert I is present in the feed stream in small quantities. A (small) purge stream P is therefore used to remove this inert from the recycle loop. The interphase mole transfer rates for the components A, B, and I in the condenser are governed by rate expressions of the form

$$N_j = \mathcal{K}_j \mathcal{A}\left(y_j - \frac{\mathcal{P}_j^S}{\mathcal{P}} x_j\right) \frac{M_L}{\rho_L}$$

where $\mathcal{K}_j\mathcal{A}$ denotes a mass transfer coefficient, y_j is the mole fraction in the gas phase, x_j is the mole fraction in the liquid phase, $\mathcal{P}_j^S$ is the saturation vapor pressure of the component j, $\mathcal{P}$ is the total pressure in the condenser, M_L is the total molar liquid holdup in the condenser, and ρ_L is the molar density of the liquid. Assuming isothermal operation, the dynamic model of the network has the form:

$$\dot{M}_R = F_o + R - F$$

$$\dot{y}_{A,R} = \frac{1}{M_R}[F_o(y_{A,o} - y_{A,R}) + R(y_A - y_{A,R})] - r_A$$

$$\dot{y}_{I,R} = \frac{1}{M_R}[F_o(y_{I,o} - y_{I,R}) + R(y_I - y_{I,R})]$$

$$\dot{M}_V = F - R - N - P$$

$$\dot{y}_A = \frac{1}{M_V}[F(y_{A,R} - y_A) - N_A + y_A N]$$

$$\dot{y}_I = \frac{1}{M_V}[F(y_{I,R} - y_I) - N_I + y_I N]$$

$$\dot{M}_L = N - L$$
$$\dot{x}_A = \frac{1}{M_L}[N_A - x_A N]$$
$$\dot{x}_I = \frac{1}{M_L}[N_I - x_I N] \quad (1)$$

where $N = N_A + N_B + N_I$ and M_R, M_V, and M_L denote the molar holdups in the reactor, vapor phase in the condenser, and liquid phase in the condenser, respectively, and $r_A = k_1 y_{A,R}$ represents the reaction rate.

In our analysis, we assume that the flow rates in the recycle loop are $O(1)$ and that for economic and operational reasons, the flow rate of the purge stream is very small. Thus, the ratio of the purge flow rate to the feed flow rate under steady-state conditions is very small, or $P_s/F_{o,s} = \varepsilon \ll 1$. Also, we consider that the mole fraction of the inert in the feed is very small, or $y_{I,o} = \beta_1 \varepsilon$, where β_1 is $O(1)$, and that the inert does not separate readily in the separation unit. Thus, we assume that the mass transfer rate for the inert component is very small, or $\mathcal{H}_I \mathcal{A} = \beta_2 \varepsilon^2$, where β_2 is $O(1)$ and that the inert is very volatile, having a high vapor pressure, or $\mathcal{P}_I^S/\mathcal{P} = \beta_3(1/\varepsilon)$, where β_3 is $O(1)$.

Note that, based on steady-state considerations, to remove an appreciable amount of the inert component from the recycle loop, the mole fraction of the inert in the vapor phase in the condenser, y_I, has to be $O(1)$. This implies that $O(\varepsilon)$ moles of inert enter and leave the system through the feed and purge streams. Note also that the two final statements, concerning the mass transfer properties of the inert component, imply that a negligible amount of inert leaves the recycle loop and exits through the liquid stream from the bottom of the condenser.

Based on the preceding assumptions, the dynamic model of the network takes the form of the following system of equations:

$$\dot{M}_R = F_o + R - F$$
$$\dot{y}_{AR} = \frac{1}{M_R}[F_o(1 - \beta_1\varepsilon - y_{A,R}) + R(y_A - y_{A,R})] - r_A$$
$$\dot{y}_{IR} = \frac{1}{M_R}[F_o(\beta_1\varepsilon - y_{I,R}) + R(y_I - y_{I,R})]$$
$$\dot{M}_V = F - R - (N_A + N_B) - \beta_2\varepsilon^2 y_I + \beta_2\beta_3\varepsilon x_I - \varepsilon F_{o,s}\frac{P}{P_s}$$
$$\dot{y}_A = \frac{1}{M_V}[F(y_{A,R} - y_A) - N_A + y_A(N_A + N_B) + y_A(\beta_2\varepsilon^2 y_I - \beta_2\beta_3\varepsilon x_I)]$$
$$\dot{y}_I = \frac{1}{M_V}[F(y_{I,R} - y_I) - (\beta_2\varepsilon^2 y_I - \beta_2\beta_3\varepsilon x_I) + y_I(N_A + N_B) + y_I(\beta_2\varepsilon^2 y_I - \beta_2\beta_3\varepsilon x_I)]$$
$$\dot{M}_L = (N_A + N_B) + \beta_2\varepsilon^2 y_I - \beta_2\beta_3\varepsilon x_I - L$$
$$\dot{x}_A = \frac{1}{M_L}[N_A - x_A(N_A + N_B) - x_A(\beta_2\varepsilon^2 y_I - \beta_2\beta_3\varepsilon x_I)]$$

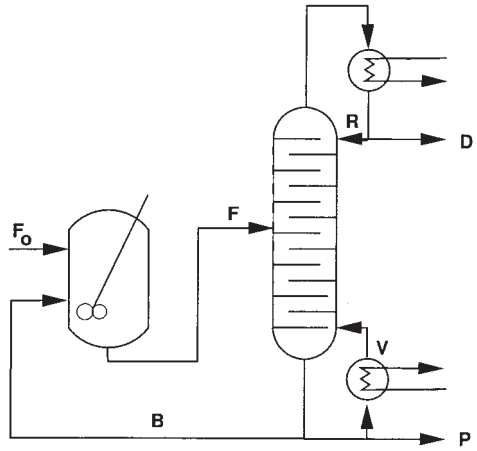

Figure 2. Reactor–distillation column process network with recycle and purge.

$$\dot{x}_I = \frac{1}{M_L}[\beta_2\varepsilon^2 y_I - \beta_2\beta_3\varepsilon x_I - x_I(N_A + N_B) - x_I(\beta_2\varepsilon^2 y_I - \beta_2\beta_3\varepsilon x_I)] \quad (2)$$

Process networks with recycle and heavy inert components

Let us now consider a process network consisting of a reactor and a distillation column with N trays, as in Figure 2. The first-order reaction

$$E \rightarrow A \quad (3)$$

takes place in the reactor. The feed F_o contains the reactant E and a small quantity of a nonvolatile, heavy inert I, and the effluent of the reactor is fed to a distillation column. We assume that the product A is light/volatile, and is removed at the top of the column, whereas the heavy reactant E is removed as bottoms and recycled to the reactor. To prevent the accumulation of the heavy inert I, a small purge stream of flow rate P is used.

Under the standard equilibrium assumptions for the tray compositions

$$y_{A,i} = \frac{\alpha_A x_{A,i}}{1 + (\alpha_I - 1)x_{I,i} + (\alpha_A - 1)x_{A,i}} \quad (4)$$

$$y_{I,i} = \frac{\alpha_I x_{I,i}}{1 + (\alpha_I - 1)x_{I,i} + (\alpha_A - 1)x_{A,i}} \quad (5)$$

where $x_{j,i}$ and $y_{j,i}$ represent, respectively, the liquid and vapor mole fractions of component j on tray i, where α_j is the relative volatility of component j, the $(2N + 9)$-dimensional model of the process network is:

$$\dot{M}_R = F_o + B - F$$
$$\dot{x}_{A,R} = \frac{1}{M_R}[F_o(x_{A,o} - x_{A,R}) + B(x_{A,B} - x_{A,R})$$

$$+ k(1 - x_{A,R} - x_{I,R})M_R]$$

$$\dot{x}_{I,R} = \frac{1}{M_R}[F_o(x_{I,o} - x_{I,R}) + B(x_{I,B} - x_{I,R})]$$

$$\dot{M}_D = V - R - D$$

$$\dot{x}_{A,D} = \frac{V}{M_D}(y_{A,1} - x_{A,D})$$

$$\dot{x}_{I,D} = \frac{V}{M_D}(y_{I,1} - x_{I,D})$$

$$\vdots$$

$$\dot{x}_{A,i} = \frac{1}{M_i}[V(y_{A,i+1} - y_{A,i}) + R(x_{A,i-1} - x_{A,i})]$$

$$\dot{x}_{I,i} = \frac{1}{M_i}[V(y_{I,i+1} - y_{I,i}) + R(x_{I,i-1} - x_{I,i})]$$

$$\vdots$$

$$\dot{x}_{A,f} = \frac{1}{M_f}[V(y_{A,f+1} - y_{A,f}) + R(x_{A,f-1} - x_{A,f}) + F(x_{A,R} - x_{A,f})]$$

$$\dot{x}_{I,f} = \frac{1}{M_f}[V(y_{I,f+1} - y_{I,f}) + R(x_{I,f-1} - x_{I,f}) + F(x_{I,R} - x_{I,f})]$$

$$\vdots$$

$$\dot{x}_{A,i} = \frac{1}{M_i}[V(y_{A,i+1} - y_{A,i}) + (R + F)(x_{A,i-1} - x_{A,i})]$$

$$\dot{x}_{I,i} = \frac{1}{M_i}[V(y_{I,i+1} - y_{I,i}) + (R + F)(x_{I,i-1} - x_{I,i})]$$

$$\vdots$$

$$\dot{M}_B = R + F - B - P$$

$$\dot{x}_{A,B} = \frac{1}{M_B}[(R + F)(x_{A,N} - x_{A,B}) + V(x_{A,B} - y_{A,B})]$$

$$\dot{x}_{I,B} = \frac{1}{M_B}[(R + F)(x_{I,N} - x_{I,B}) + V(x_{I,B} - y_{I,B})] \qquad (6)$$

As discussed earlier, we consider that the flow rates in the recycle loop are $O(1)$ and that the flow rate of the purge stream is very small compared to the network throughput, that is, $P_s/F_{o,s} = \varepsilon \ll 1$. Also, we consider that the mole fraction of the inert in the feed stream is very small $y_{I,o} = \beta_1\varepsilon$, where β_1 is $O(1)$and the subscript s denotes nominal values. Because the inert is heavy and is recycled with the column bottoms, we assume that it has a high boiling point, or, equivalently, a low relative volatility. More specifically, $\alpha_I = \beta_2\varepsilon^2$, where the β_2 term is $O(1)$.

Under the preceding considerations, the phase equilibrium Eq. 4 system becomes

$$y_{A,i} = \frac{\alpha_A x_{A,i}}{\mathcal{N}} \qquad y_{I,i} = \frac{\varepsilon^2\beta_2 x_{I,i}}{\mathcal{N}} \qquad (7)$$

with

$$\mathcal{N} = 1 + (\varepsilon^2\beta_2 - 1)x_{I,i} + (\alpha_A - 1)x_{A,i}$$

and the network model takes the form of the following system of equations:

$$\dot{M}_R = F_o + B - F$$

$$\dot{x}_{A,R} = \frac{1}{M_R}[F_o(1 - \beta_1\varepsilon - x_{A,R}) + B(x_{A,B} - x_{A,R}) + k(1 - x_{A,R} - x_{I,R})M_R]$$

$$\dot{x}_{I,R} = \frac{1}{M_R}[F_o(\beta_1\varepsilon - x_{I,R}) + B(x_{I,B} - x_{I,R})]$$

$$\dot{M}_D = V - R - D$$

$$\dot{x}_{A,D} = \frac{V}{M_D}(y_{A,1} - x_{A,D})$$

$$\dot{x}_{I,D} = \frac{V}{M_D}\left(\frac{\varepsilon^2\beta_2 x_{I,1}}{\mathcal{N}} - x_{I,D}\right)$$

$$\vdots$$

$$\dot{x}_{A,i} = \frac{1}{M_i}[V(y_{A,i+1} - y_{A,i}) + R(x_{A,i-1} - x_{A,i})]$$

$$\dot{x}_{I,i} = \frac{1}{M_i}\left[V\left(\frac{\varepsilon^2\beta_2 x_{I,i+1}}{\mathcal{N}} - \frac{\varepsilon^2\beta_2 x_{I,i}}{\mathcal{N}}\right) + R(x_{I,i-1} - x_{I,i})\right]$$

$$\vdots$$

$$\dot{x}_{A,f} = \frac{1}{M_f}[V(y_{A,f+1} - y_{A,f}) + R(x_{A,f-1} - x_{A,f}) + F(x_{A,R} - x_{A,f})]$$

$$\dot{x}_{I,f} = \frac{1}{M_f}\left[V\left(\frac{\varepsilon^2\beta_2 x_{I,f+1}}{\mathcal{N}} - \frac{\varepsilon^2\beta_2 x_{I,f}}{\mathcal{N}}\right) + R(x_{I,f-1} - x_{I,f}) + F(x_{I,R} - x_{I,f})\right]$$

$$\vdots$$

$$\dot{x}_{A,i} = \frac{1}{M_i}[V(y_{A,i+1} - y_{A,i}) + (R + F)(x_{A,i-1} - x_{A,i})]$$

$$\dot{x}_{I,i} = \frac{1}{M_i}\left[V\left(\frac{\varepsilon^2\beta_2 x_{I,i+1}}{\mathcal{N}} - \frac{\varepsilon^2\beta_2 x_{I,i}}{\mathcal{N}}\right) + (R + F)(x_{I,i-1} - x_{I,i})\right]$$

$$\vdots$$

$$\dot{M}_B = R + F - B - V - \varepsilon F_{o,s}\frac{P}{P_s}$$

$$\dot{x}_{A,B} = \frac{1}{M_B}[(R + F)(x_{A,N} - x_{A,B}) + V(x_{A,B} - y_{A,B})]$$

$$\dot{x}_{I,B} = \frac{1}{M_B}\left[(R + F)(x_{I,N} - x_{I,B}) + V\left(x_{I,B} - \frac{\varepsilon^2\beta_2 x_{I,B}}{\mathcal{N}}\right)\right] \qquad (8)$$

It is evident that the above models (Eqs. 2 and 8) have terms of $O(1)$ and $O(\varepsilon)$, which suggests, potentially, a two-time scale behavior for the process networks with recycle and purge streams that they describe. In the next section, we develop a generic modeling framework for such networks that captures this feature and allows for a more general analysis of their dynamic behavior.

Modeling of Process Networks with Recycle and Purge

We consider the class of process networks presented in Figure 3, consisting of N units and a total of C components and a single recycle loop. We consider that a separator is present and we denote by S the part of the separator that is included in the recycle loop, and by $S + 1$ the part that is outside the loop. We consider that one of the output streams of the separator is

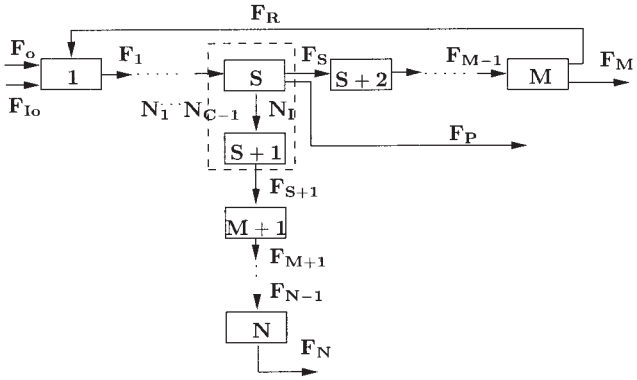

Figure 3. Generic reactor–separator process network with recycle and purge.

at least partially recycled (possibly through units $S+2\cdots M$), whereas the other output stream leaves the network as a product stream, potentially after being processed in units $M+1\cdots N$. An impurity I is introduced in the network at a small rate, and we assume that it does not separate readily in the separator. A purge stream is used to prevent the accumulation of the impurity in the recycle loop.

Let F_o denote the feed flow rate to the first unit; F_{Io} the rate at which the impurity is input to the network; F_j ($j=1,\ldots,N$), the outlet flow rate from the jth unit; F_R the recycle flow rate; and F_P the purge flow rate. Also, let N_i ($i=1,\ldots,C-1$) and N_I denote the net rate at which the ith component and the impurity, respectively, are separated from the recycle loop.

Considering that the individual process units are modeled as lumped parameters systems, the mathematical model that describes the overall and component material balances of the network takes the form

$$\dot{\mathbf{x}} = \mathbf{f}(\mathbf{x}) + \sum_{j=1}^{N} \mathbf{g}_j(\mathbf{x}) F_j + \sum_{i=1}^{C-1} \mathbf{g}_{c,i}(\mathbf{x}) N_i + \mathbf{g}_R(\mathbf{x}) F_R + \mathbf{g}_{Io}(\mathbf{x}) F_{Io} + \mathbf{g}_I(\mathbf{x}) N_I + \mathbf{g}_P(\mathbf{x}) F_P \quad (9)$$

where $\mathbf{x} \subset \mathcal{X} \in \mathbb{R}^n$ represents the state vector and $\mathbf{f}(\mathbf{x})$, $\mathbf{g}_j(\mathbf{x})$, $\mathbf{g}_{c,i}(\mathbf{x})$, $\mathbf{g}_R(\mathbf{x})$, $\mathbf{g}_{Io}(\mathbf{x})$, $\mathbf{g}_I(x)$, and $\mathbf{g}_P(x)$ are appropriately defined n-dimensional vector functions.

We assume that the following properties of the network are valid:

Assumption A-1 *The nominal flow rate of the purge stream is much smaller than that of the feed stream, that is,*

$$F_{P,s}/F_{o,s} = \varepsilon \ll 1$$

where the subscript s denotes nominal steady state values.

Assumption A-2 *The rate at which the impurity is input to the network is very small, that is,*

$$F_{Io,s}/F_{o,s} = \beta_1 \varepsilon$$

where β_1 is $O(1)$.

Assumption A-3 *The net rate of impurity removal from the recycle loop by the product stream separated in the separation unit (along the path $N_I, F_{S+1}, \ldots, F_N$) is much smaller than the rate at which the impurity is input to the network:*

$$N_{I,s}/F_{o,s} = \beta_2 \varepsilon^2$$

where β_2 is an $O(1)$ quantity.

Assumption A-4 *The flow rates $F_o, \ldots, F_N, F_R$ and $N_1, \ldots, N_{C-1}$ are of comparable magnitude, that is*

$$\frac{F_{j,s}}{F_{o,s}} = O(1) \qquad \frac{N_{i,s}}{F_{o,s}} = O(1)$$

We denote $u_{c,i} = N_i/N_{i,s}$, $i=1,\ldots,C-1, I$. Also, we define $u_j = F_j/F_{js}$ to be the scaled (possibly manipulated) inputs that correspond to the flow rates F_j.

Under Assumptions A-1 to A-4, the generic model in Eq. 9 becomes

$$\dot{\mathbf{x}} = \mathbf{f}(\mathbf{x}) + \sum_{j=1}^{N} \mathbf{g}_j(\mathbf{x}) F_{j,s} u_j + \sum_{i=1}^{C-1} \mathbf{g}_{c,i}(\mathbf{x}) N_{i,s} u_{c,i} + \mathbf{g}_R(\mathbf{x}) F_{R,s} u_R + \varepsilon[\mathbf{g}_{Io}(\mathbf{x}) F_{o,s} \beta_1 + \varepsilon \mathbf{g}_I(\mathbf{x}) F_{o,s} u_{c,I} \beta_2 + \mathbf{g}_P(\mathbf{x}) F_{o,s} u_p] \quad (10)$$

Equation 10 can be written in a more compact form as

$$\dot{\mathbf{x}} = \bar{\mathbf{f}}(\mathbf{x}, \mathbf{u}^I) + \varepsilon[\mathbf{g}^{Io}(\mathbf{x}) + \varepsilon \mathbf{g}^I(\mathbf{x}) + \mathbf{g}^P(\mathbf{x}) u_p] \quad (11)$$

where $\mathbf{u}^I$ is the vector of scaled input variables corresponding to the "large" flow rates $F_o, \ldots, F_N, F_R$ and $\bar{\mathbf{f}}(\mathbf{x}, \mathbf{u}^I)$, $\mathbf{g}^{Io}(\mathbf{x})$, $\mathbf{g}^I(\mathbf{x})$, and $\mathbf{g}^P(\mathbf{x})$ are n-dimensional vector functions. Notice that the flow rates $u_{c,i}$ are generally defined as functions of the physical parameters of the system, that is, $u_{c,i} = u_{c,i}(\mathbf{x})$, and thus the corresponding terms have been included in the expressions of $\bar{\mathbf{f}}(\mathbf{x}, \mathbf{u}^I)$ and $\mathbf{g}^I(\mathbf{x})$.

The above description captures the material balance models of typical reaction separation process networks with recycle and purge, such as the process networks considered in the second section. Because of the presence of terms of vastly different [$O(1)$ and $O(\varepsilon)$] magnitudes, it is possible that the networks of the type of Eq. 11 possess a two-time scale dynamics. Furthermore, notice that Eq. 11 is in a *nonstandard* singularly perturbed form, that is, there is no explicit separation of the state variables into "fast" and "slow." Generally, in such cases, all the states $\mathbf{x}$ will exhibit an initial fast transience, succeeded by slow dynamics. In what follows, we show, within the framework of singular perturbations, that such networks exhibit indeed a two-time scale dynamic behavior. Moreover, we address the derivation of reduced-order models of the fast and slow dynamics of the network.

Model Reduction and Control Implications

We proceed by considering the limiting case of the purge flow rate being set to zero, that is, $\varepsilon \to 0$. In this limit, we obtain a description of the fast dynamics of the network:

$$\dot{\mathbf{x}} = \bar{\mathbf{f}}(\mathbf{x}, \mathbf{u}^l) \tag{12}$$

The description of the fast dynamics in Eq. 12 involves only the flow rates $\mathbf{u}^l$. However, it is easy to verify that these flow rates do not affect the *total holdup* of the impurity in the recycle loop. The total holdup of I is influenced only by the inflow of impurity, its transfer rate in the separator, and the purge stream, which, as can be seen from Eq. 12, have no influence on the dynamics in the fast time scale. Consequently, one of the differential equations describing the fast dynamics is redundant, and the equation in Eq. 12 are not independent. Equivalently, the steady-state conditions

$$\mathbf{0} = \bar{\mathbf{f}}(\mathbf{x}, \mathbf{u}^l) \tag{13}$$

do not specify a set of isolated equilibrium points for the fast dynamics, but rather a one-dimensional equilibrium manifold, in which a slow dynamics will evolve. The vector function $\bar{\mathbf{f}}$ can be reformulated[9,13] as

$$\bar{\mathbf{f}}(\mathbf{x}, \mathbf{u}^l) = \mathbf{B}(\mathbf{x})\tilde{\mathbf{f}}(\mathbf{x}, \mathbf{u}^l) \tag{14}$$

where $\mathbf{B}(\mathbf{x}) \in \mathbb{R}^{n\times(n-1)}$ is a full-column rank matrix and the vector $\tilde{\mathbf{f}}(\mathbf{x}, \mathbf{u}^l) \in \mathbb{R}^{n-1}$ has linearly independent terms.

Next, to obtain a description of the slow dynamics, we define a slow, *compressed*, time scale $\tau = \varepsilon t$, in which the model of the process network becomes

$$\varepsilon \frac{d\mathbf{x}}{d\tau} = \bar{\mathbf{f}}(\mathbf{x}, \mathbf{u}^l) + \varepsilon[\mathbf{g}^{Io}(\mathbf{x}) + \varepsilon\mathbf{g}^I(\mathbf{x}) + \mathbf{g}^P(\mathbf{x})u_p] \tag{15}$$

and we consider the limit $\varepsilon \to 0$, in which the constraints $\mathbf{0} = \bar{\mathbf{f}}(\mathbf{x}, \mathbf{u}^l)$, or, equivalently, the linearly independent constraints $\mathbf{0} = \tilde{\mathbf{f}}(\mathbf{x}, \mathbf{u}^l)$ are obtained. These constraints are essentially the quasi-steady-state conditions for the fast dynamics in Eqs. 13 and 14 and must be satisfied in the slow time scale.

Dividing Eq. 15 by ε, and considering the same limiting case under the preceding constraints, we obtain a description of the slow dynamics of the system. Note that, in this limit, the term $\tilde{\mathbf{f}}(\mathbf{x}, \mathbf{u}^l)/\varepsilon$ becomes indeterminate. By defining $\mathbf{z} = \lim_{\varepsilon\to 0} \tilde{\mathbf{f}}(\mathbf{x}, \mathbf{u}^l)/\varepsilon$, $\mathbf{z} \in \mathbb{R}^{n-1}$, as this finite but unknown term, the slow dynamics of network Eq. 11 takes the form

$$\frac{d\mathbf{x}}{d\tau} = \mathbf{g}^{Io}(\mathbf{x}) + \mathbf{g}^P(\mathbf{x})u_p + \mathbf{B}(\mathbf{x})\mathbf{z}$$

$$\mathbf{0} = \tilde{\mathbf{f}}(\mathbf{x}, \mathbf{u}^l) \tag{16}$$

The model of the slow dynamics of the system thus constitutes a set of coupled differential and algebraic equations (DAEs) of nontrivial index because the variables $\mathbf{z}$ (that physically correspond to the net material flows of the network in the slow time scale) are implicitly fixed by the quasi-steady-state constraints, rather than explicitly specified in the dynamic model. Also, note that the DAE model Eq. 16 has a well-defined index only if the flow rates $\mathbf{u}^l$ that appear in the algebraic constraints that determine the constrained state–space are specified as functions of the state variables $\mathbf{x}$, by a control law $\mathbf{u}^l(\mathbf{x})$.

Once the flow rates $\mathbf{u}^l$ are specified by appropriate control laws, it is possible to differentiate the constraints in Eq. 16 to obtain (after differentiating a sufficient number of times) a solution for the algebraic variables $\mathbf{z}$. One differentiation in time will yield

$$\mathbf{z} = -[L_{\mathbf{B}}\tilde{\mathbf{f}}(\mathbf{x})]^{-1}[L_{\mathbf{g}^{Io}}\tilde{\mathbf{f}}(\mathbf{x}) + L_{\mathbf{g}^P}\tilde{\mathbf{f}}(\mathbf{x})u^P] \tag{17}$$

with

$$L_{\mathbf{B}}\tilde{\mathbf{f}}(\mathbf{x}) = \frac{\partial\tilde{\mathbf{f}}}{\partial\mathbf{x}}\mathbf{B}(\mathbf{x}) \qquad L_{\mathbf{g}^{Io}}\tilde{\mathbf{f}}(\mathbf{x}) = \frac{\partial\tilde{\mathbf{f}}}{\partial\mathbf{x}}\mathbf{g}^{Io}\; L_{\mathbf{g}^P}\tilde{\mathbf{f}}(\mathbf{x}) = \frac{\partial\tilde{\mathbf{f}}}{\partial\mathbf{x}}\mathbf{g}^P$$

If the matrix $L_{\mathbf{B}}\tilde{\mathbf{f}}$ is invertible (which is typically true; see the examples that follow), the index of the DAE system Eq. 16 is 2 (that is, a solution for $\mathbf{z}$ is obtained from Eq. 17), and in this case the dimension of the underlying ODE system describing the slow dynamics is 1.

In this case, an explicit ODE representation (state–space realization) of the DAE system Eq. 16 can be obtained be using a coordinate change of the form

$$\begin{bmatrix}\zeta\\ \boldsymbol{\eta}\end{bmatrix} = \mathbf{T}(\mathbf{x}) = \begin{bmatrix}\phi(\mathbf{x})\\ \tilde{\mathbf{f}}(\mathbf{x}, \mathbf{u}^l)\end{bmatrix} \tag{18}$$

In these new coordinates, the model of the slow dynamics becomes

$$\frac{d\zeta}{d\tau} = \frac{\partial\phi}{\partial\mathbf{x}}\mathbf{B}(\mathbf{x})\mathbf{z}\big|_{\mathbf{x}=\mathbf{T}^{-1}(\zeta)} + \frac{\partial\phi}{\partial\mathbf{x}}\mathbf{g}^{Io}(\mathbf{x})\big|_{\mathbf{x}=\mathbf{T}^{-1}(\zeta)} + \frac{\partial\phi}{\partial\mathbf{x}}\mathbf{g}^P(\mathbf{x})u^P\big|_{\mathbf{x}=\mathbf{T}^{-1}(\zeta)}$$
$$\boldsymbol{\eta} \equiv \mathbf{0} \tag{19}$$

Furthermore, it is possible to choose the function $\phi(\mathbf{x})$ so that $(\partial\phi/\partial\mathbf{x})\mathbf{B}(\mathbf{x}) = 0$.[14]. In this case, the variable ζ evolves independently of the variables $\mathbf{z}$, and represents a *true "slow" variable* in the system (whereas the original state variables exhibit both fast and slow dynamics). Its dynamics is given by

$$\frac{d\zeta}{d\tau} = \frac{\partial\phi}{\partial\mathbf{x}}\mathbf{g}^{Io}(\mathbf{x})\big|_{\mathbf{x}=\mathbf{T}^{-1}(\zeta)} + \frac{\partial\phi}{\partial\mathbf{x}}\mathbf{g}^P(\mathbf{x})u^p\big|_{\mathbf{x}=\mathbf{T}^{-1}(\zeta)}$$
$$\boldsymbol{\eta} \equiv \mathbf{0} \tag{20}$$

Remark 1 The analysis presented above also has implications on the selection of control structures for process networks with recycle and purge. As it was shown, it allows for a separation of the available flow rates into two distinct sets of manipulated inputs, that act on and can be used to address control objectives in the two time scales. Specifically, $\mathbf{u}^l$ are to be used to address control objectives (such as stabilization of holdups and product purity) in the fast time scale, whereas the flow rate u^P of the small purge stream is to be used for controlling the slow dynamics of the impurity levels in the network.

Remark 2 Assumption A-4 can be relaxed to consider process networks in which flow rates of several distinct magnitudes are present. In the case of process networks with small purge

streams, where the recycle flow rate is much larger than the throughput, the general model (Eq. 11) becomes

$$\dot{\mathbf{x}} = \mathbf{f}(\mathbf{x}) + \mathbf{g}^s\mathbf{u}^s + \frac{1}{\varepsilon_1}\mathbf{g}^l\mathbf{u}^l + \varepsilon_2[\mathbf{g}^{l_o}(\mathbf{x}) + \varepsilon_2\mathbf{g}^l(\mathbf{x}) + \mathbf{g}^P(\mathbf{x})u_p] \tag{21}$$

where $\mathbf{u}^s$ and $\mathbf{u}^l$ denote, respectively, the network feed and product flow rates, and the large internal and recycle flow rates. In Eq. 21, $\varepsilon_1 = F_{o,s}/F_{R,s} \ll 1$, capturing the fact that the recycle flow rate, although comparable in magnitude to flow rates of the internal streams, is assumed to be much larger than the network throughput. $\varepsilon_2 = P_s/F_{o,s} \ll 1$ represents the ratio of the nominal flow rate of the small purge stream and of the network throughput, as defined above. Evidently, the Eq. 21 model contains terms of $O(1)$, $O(\varepsilon)$, and $O(1/\varepsilon)$, suggesting potentially a three-time scale behavior.

Motivating Examples II

We now continue with the analysis of the motivating examples introduced in the second section, and present the derivation of reduced-order models for the fast and slow dynamics of the two process networks, according to the theoretical framework developed above.

Process networks with light inerts

We begin with a description of the fast dynamics of the stiff model in Eq. 2. This is readily obtained in the form of Eq. 12 by considering the dynamic model (Eq. 2) in the limit as $\varepsilon \to 0$:

$$\begin{aligned}
\dot{M}_R &= F_o + R - F \\
\dot{y}_{A,R} &= \frac{1}{M_R}[F_o(1 - y_{A,R}) + R(y_A - y_{A,R})] - r_A \\
\dot{y}_{I,R} &= \frac{1}{M_R}[-F_o y_{I,R} + R(y_I - y_{I,R})] \\
\dot{M}_V &= F - R - (N_A - N_B) \\
\dot{y}_A &= \frac{1}{M_V}[F(y_{A,R} - y_A) - N_A + y_A(N_A + N_B)] \\
\dot{y}_I &= \frac{1}{M_V}[F(y_{I,R} - y_I) + y_I(N_A + N_B)] \\
\dot{N}_L &= (N_A + N_B) - L \\
\dot{x}_A &= \frac{1}{M_L}[N_A - x_A(N_A + N_B)] \\
\dot{x}_I &= -\frac{1}{M_L}[x_I(N_A + N_B)]
\end{aligned} \tag{22}$$

Equation 22 is a nonstiff model that approximates the dynamics of the reactor–condenser network in Figure 1 in the original (fast) time scale t.

Note that the differential equations in the Eq. 22 system are not independent, or, equivalently, the corresponding quasi-steady-state constraints are not linearly independent. Specifically, the third constraint can be expressed as a linear combination of the others, that is, there are only eight linearly independent constraints, that can be written in the form of Eq. 14, with

$$\mathbf{B}(\mathbf{x}) = \begin{bmatrix}
1 & 0 & 0 & 0 & 0 & 0 & 0 & 0 \\
0 & \frac{1}{M_R} & 0 & 0 & 0 & 0 & 0 & 0 \\
-\frac{y_{I,R}}{M_R} & 0 & -\frac{y_I}{M_R} & 0 & -\frac{1}{M_R} & 0 & 0 & 0 \\
0 & 0 & 1 & 0 & 0 & 0 & 0 & 0 \\
0 & 0 & 0 & \frac{1}{M_V} & 0 & 0 & 0 & 0 \\
0 & 0 & 0 & 0 & \frac{1}{M_V} & 0 & 0 & 0 \\
0 & 0 & 0 & 0 & 0 & 1 & 0 & 0 \\
0 & 0 & 0 & 0 & 0 & 0 & \frac{1}{M_L} & 0 \\
0 & 0 & 0 & 0 & 0 & 0 & 0 & \frac{1}{M_L}
\end{bmatrix} \tag{23}$$

and

$$\tilde{\mathbf{f}}(\mathbf{x}, \mathbf{u}^l) = \begin{bmatrix}
F_o + R - F \\
F_o(1 - y_{A,R}) + R(y_A - y_{A,R}) - r_A M_R \\
F - R - (N_A + N_B) \\
F(y_{A,R} - y_A) - N_A + y_A(N_A + N_B) \\
F(y_{I,R} - y_I) + y_I(N_A + N_B) \\
(N_A + N_B) - L \\
N_A - x_A(N_A + N_B) \\
x_I(N_A + N_B)
\end{bmatrix} \tag{24}$$

This is consistent with the fact that these constraints correspond to the limit as the purge flow rate and the inflow of the inert become zero. In this limit, the numbers of moles of the inert component leaving the reactor and the condenser are identical, and thus the redundant constraint. Note also that in the fast time scale, only the flow rates F, R, and L affect the dynamics and can be used for addressing control objectives such as stabilization of holdups, production rate, and product quality; of course, the purge flow rate has no effect on the dynamics in this fast time scale.

Turning now to the slow dynamics, we define the slow time scale $\tau = t\varepsilon$ and consider the limit $\varepsilon \to 0$, obtaining a description of the slow dynamics of the form (Eq. 16)

$$\begin{aligned}
\frac{dM_R}{d\tau} &= \lim_{\varepsilon\to 0}\frac{1}{\varepsilon}(F_o + R - F) \\
\frac{dy_{A,R}}{d\tau} &= \lim_{\varepsilon\to 0}\frac{1}{\varepsilon M_R}[F_o(1 - y_{A,R}) + R(y_A - y_{A,R}) - r_A M_R] \\
&\quad - \frac{1}{M_R}F_o\beta_1 \\
\frac{dy_{I,R}}{d\tau} &= \lim_{\varepsilon\to 0}\frac{1}{\varepsilon M_R}[-F_o y_{I,R} + R(y_I - y_{I,R})] + \frac{1}{M_R}F_o\beta_1 \\
\frac{dM_V}{d\tau} &= \lim_{\varepsilon\to 0}\frac{1}{\varepsilon}[F - R - (N_A + N_B)] - F_{o,s}\frac{P}{P_s}
\end{aligned}$$

$$\frac{dy_A}{d\tau} = \lim_{\varepsilon\to 0}\frac{1}{\varepsilon M_V}[F(y_{A,R}-y_A)-N_A+y_A(N_A+N_B)]$$
$$\frac{dy_I}{d\tau} = \lim_{\varepsilon\to 0}\frac{1}{\varepsilon M_V}[F(y_{I,R}-y_I)+y_I(N_A+N_B)]$$
$$\frac{dM_L}{d\tau} = \lim_{\varepsilon\to 0}\frac{1}{\varepsilon}[N_A+N_B-L]$$
$$\frac{dx_A}{d\tau} = \lim_{\varepsilon\to 0}\frac{1}{\varepsilon M_L}[N_A-x_A(N_A+N_B)]$$
$$\frac{dx_I}{d\tau} = \lim_{\varepsilon\to 0}\frac{-1}{\varepsilon M_L}[x_I(N_A+N_B)] \qquad (25)$$

subject to the quasi-steady-state constraints obtained by setting the terms in Eq. 24 equal to zero.

It was verified that by setting the reactor effluent flow rate F and the product flow rate L with the proportional control laws

$$F = F_s[1-k_{p,1}(M_{R,sp}-M_R)]$$
$$L = L_s[1-k_{p,2}(M_{L,sp}-M_L)] \qquad (26)$$

where the index s denotes nominal values and the index sp denotes set points, the matrix $L_{\mathbf{B}}\tilde{\mathbf{f}}(\mathbf{x})$ is invertible, and thus a coordinate change of the Eq. 18 type exists. Note that the control laws in Eq. 26 correspond to the stabilization of the reactor and condenser liquid holdups.

To obtain an ODE description of the slow dynamics, a meaningful choice of the function $\phi(\mathbf{x})$in Eq. 18 is

$$\phi(x) = M_R y_{I,R} + M_V y_I$$

that is, the total inert holdup in the recycle loop. This choice of coordinate change yields the following state–space realization of the slow dynamics of the network in Figure 1:

$$\frac{d\zeta}{d\tau} = F_0\beta_1 - F_{0,s}\frac{P}{P_s}y_I(\zeta) \qquad (27)$$

where $y_I(\zeta)$ is computed from the steady-state constraints obtaining by setting $\tilde{\mathbf{f}}(\mathbf{x}, \mathbf{u}^l)$ in Eq. 24 equal to zero and inverting the coordinate transformation (Eq. 18), with ζ defined as above. Equation 27 represents a one-dimensional, nonstiff description of the slow dynamics of the process network in Figure 1. The single slow mode of the network is therefore associated with the total holdup of the inert impurity, which is a "true slow variable" of the network.

Process networks with recycle and heavy inert components

Following a similar procedure to the one used above, it is easy to verify that we obtain a model that approximates the fast dynamics of the network in Figure 2, that is in the form of Eq. 12. Also, it can be verified that only $2N + 8$ of the $2N + 9$ steady-state constraints that correspond to the fast dynamics are independent. After controlling the reactor holdup M_R, the distillate holdup M_D, and the reboiler holdup M_B with proportional controllers using, respectively, F, D, and B as manipulated inputs, the matrix $L_{\mathbf{B}}\tilde{\mathbf{f}}(\mathbf{x})$ is nonsingular, and thus the coordinate change

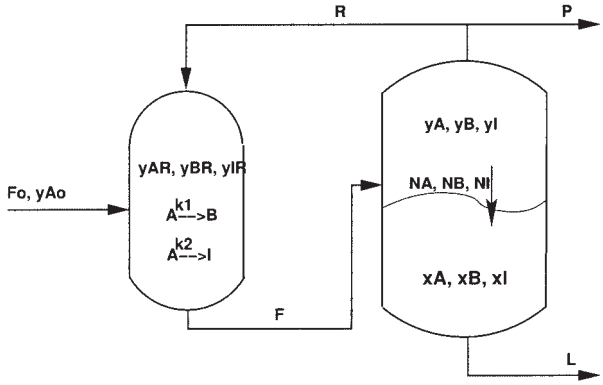

Figure 4. Process network in which a secondary reaction takes place, yielding small quantities of an unwanted byproduct.

$$\zeta = M_R x_{I,R} + M_f x_{I,f} + M_B x_{I,B} + \sum_{i=f+1}^{N} M_i x_{I,i} \qquad (28)$$

which corresponds to the total holdup of the impurity in the recycle loop. After applying Eq. 28, we obtain the following one-dimensional description of the slow dynamics of the network:

$$\frac{d\zeta}{d\tau} = \beta_1 F_o - F_{o,s}\frac{P}{P_s}x_{I,B}(\zeta) \qquad (29)$$

Similar to the previous example we considered, the total holdup of the impurity represents is the "true slow variable" that the one-dimensional slow dynamics of the network is associated with.

Remarks

Slow secondary reactions

An analysis similar to those presented above can be carried out in the case of a process network in which the "impurities" are generated in the reactor, rather than introduced in the feed stream. Let us consider the process network in Figure 4, having a structure very similar to that of the reactor–condenser network presented in the second section. The difference consists in the fact that two first-order reactions $A \to B$ and $A \to I$ take place in the reactor, with reaction rate constants k_1 and k_2, respectively. B is the desired product and is separated in the condenser, whereas the undesired light byproduct I (which is assumed to be produced in small quantities) does not separate and a purge stream P is used for its removal. Carrying over the notation and modeling assumptions of the second section, the model of the process network in Figure 4 becomes

$$\dot{M}_R = F_o + R - F$$
$$\dot{y}_{A,R} = \frac{1}{M_R}[F_o(y_{Ao}-y_{A,R}) + R(y_A - y_{A,R}) - k_1 M_R y_{A,R} - k_2 M_R y_{A,R}]$$

Table 1. Nominal Values for the Process Parameters

F_o	100.00	mol/min
R	100.00	mol/min
F	200.00	mol/min
L	97.1	mol/min
P	3.9	mol/min
$y_{A,o}$	0.98	
$y_{I,o}$	0.02	
$k_{p,1}$	0.01	min^{-1}
$k_{p,2}$	0.01	min^{-1}
V_c	2.00	m^3
T_c	279.00	K
P_c	2.83	MPa
$\mathcal{A}$	200.00	m^2/m^3
$\mathcal{H}_A$	342.00	mol/m^2 min
$\mathcal{H}_B$	360.00	mol/m^2 min
$\mathcal{H}_I$	1.8×10^{-5}	mol/m^2 min
$\mathcal{P}_A^S(T_c)$	4.00	MPa
$\mathcal{P}_B^S(T_c)$	0.80	MPa
$\mathcal{P}_I^S(T_c)$	90.00	MPa
ρ_I	15.00	kmol/m^3
M_R	2412.0	mol
M_V	1228.0	mol
M_L	14,940.0	mol
y_A	0.219	
y_I	0.266	
$y_{A,R}$	0.255	
$y_{I,R}$	0.512	
x_A	0.181	
x_I	1.91×10^{-5}	

*The subscript c indicates process parameters for the condenser.

$$\dot{y}_{I,R} = \frac{1}{M_R}\left[-F_o y_{I,R} + R(y_I - y_{I,R}) + k_2 M_R y_{A,R}\right]$$
$$\dot{M}_V = F - R - N - P$$
$$\dot{y}_A = \frac{1}{M_V}\left[F(y_{A,R} - y_A) - N_A + y_A N\right]$$
$$\dot{y}_I = \frac{1}{M_V}\left[F(y_{I,R} - y_I) - N_I + y_I N\right]$$
$$\dot{M}_L = N - L$$
$$\dot{x}_A = \frac{1}{M_L}\left[N_A - x_A N\right]$$
$$\dot{x}_I = \frac{1}{M_L}\left[N_I - x_I N\right] \tag{30}$$

In this case, the form of Assumptions A-1 and A-3 remains the same as in the second section, whereas Assumption A-2 implies that the rate constant of the reaction that leads to the formation of the impurity is very small, or $k_2 M_{R,s}/F_{o,s} = \beta_1 \varepsilon$, where β_1 is an $O(1)$ quantity. Notice that here Assumption A-2 is expressed as a ratio of the characteristic time for the chemical reaction and the characteristic time for convection, thus being equivalent to considering that the second reaction has a low Damköhler number.

With the aforementioned assumptions, the dynamic model of the network takes the form

$$\dot{M}_R = F_o + R - F$$
$$\dot{y}_{AR} = \frac{1}{M_R}\left[F_o(y_{Ao} - y_{A,R}) + R(y_A - y_{A,R}) - k_1 M_R y_{A,R} - \varepsilon\beta_1 \frac{F_{o,s}}{M_{R,s}} M_R y_{A,R}\right]$$
$$\dot{y}_{IR} = \frac{1}{M_R}\left[-F_o y_{I,R} + R(y_I - y_{I,R}) + \varepsilon\beta_1 \frac{F_{o,s}}{M_{R,s}} M_R y_{A,R}\right]$$
$$\dot{M}_V = F - R - (N_A + N_B) - \beta_2\varepsilon^2 y_I + \beta_2\beta_3\varepsilon x_I - \varepsilon F_{o,s}\frac{P}{P_s}$$
$$\dot{y}_A = \frac{1}{M_V}\left[F(y_{A,R} - y_A) - N_A + y_A(N_A + N_B) + y_A(\beta_2\varepsilon^2 y_I - \beta_2\beta_3\varepsilon x_I)\right]$$
$$\dot{y}_I = \frac{1}{M_V}\left[F(y_{I,R} - y_I) - (\beta_2\varepsilon^2 y_I - \beta_2\beta_3\varepsilon x_I) + y_I(N_A + N_B) + y_I(\beta_2\varepsilon^2 y_I - \beta_2\beta_3\varepsilon x_I)\right]$$
$$\dot{M}_L = (N_A + N_B) + \beta_2\varepsilon^2 y_I - \beta_2\beta_3\varepsilon x_I - L$$
$$\dot{x}_A = \frac{1}{M_L}\left[N_A - x_A(N_A + N_B) - x_A(\beta_2\varepsilon^2 y_I - \beta_2\beta_3\varepsilon x_I)\right]$$
$$\dot{x}_I = \frac{1}{M_L}\left[\beta_2\varepsilon^2 y_I - \beta_2\beta_3\varepsilon x_I - x_I(N_A + N_B) - x_I(\beta_2\varepsilon^2 y_I - \beta_2\beta_3\varepsilon x_I)\right] \tag{31}$$

which is in the generic form of Eq. 11.

After applying (detailed derivations are not presented for the sake of brevity) the model reduction proposed above, considering again the total holdup of the impurity as a one-dimensional function required by the coordinate change (Eq. 18) we obtained the following state–space realization of the slow dynamics of the network in Figure 4:

$$\frac{d\zeta}{d\tau} = \frac{F_{o,s}}{M_{R,s}}\beta_1 M_R(\zeta)\, y_{A,R}(\zeta) - F_{o,s}\frac{P}{P_s}\, y_I(\zeta) \tag{32}$$

where $M_R(\zeta)$, $y_{A,R}(\zeta)$, and $y_I(\zeta)$ are computed as in the case of the reactor condenser network with feed impurities.

Analogies with networks with large recycle

Note that in the analyses presented above, the mole fractions of the impurity in the recycle loop are $O(1)$, and thus the amount of inert that is recycled in the network is much larger than the inert throughput of the network. The presence of a single slow mode associated with the inert is therefore in complete agreement with the analysis of networks with large recycle introduced in Kumar and Daoutidis,[9] which predicts a slow model of dimension equal to the number of components in the recycle loop for which the recycle flow rate is much larger than the throughput.

Simulation Case Study

In what follows we consider a network of the form shown in Figure 1 and, in addition to the model features introduced earlier, we assume that the component I acts as a reaction

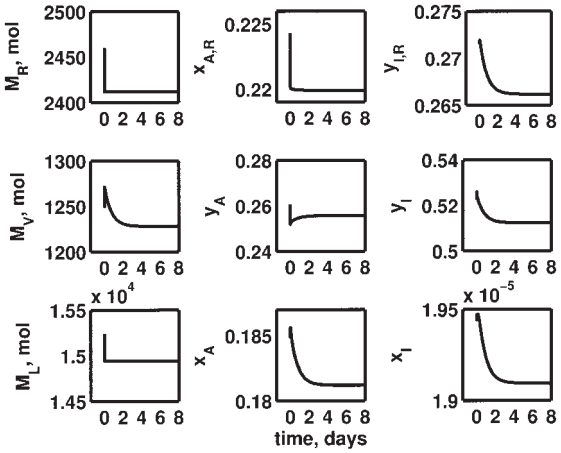

Figure 5. Time responses of all state variables.

inhibitor. Thus, the reaction rate in Eq. 1 is given by the expression

$$r_A = \frac{k_1 y_{A,R}}{1 + y_{I,R}} \tag{33}$$

The parameter values and the nominal steady states used in the case study are given in Table 1. The operating objective for this network is to control the purity of the product B at $x_{B,sp} = 0.818$, in the presence of disturbances in the inlet composition and changes in the production rate.

As an initial simulation run, we considered an "open-loop" experiment, whereby only the proportional controllers (Eq. 26) are implemented to stabilize the holdups of the network, and we slightly perturbed the state variables from their steady-state values. The corresponding responses are presented in Figure 5. Observe that the state variables exhibit a fast transient, followed by a slow approach to steady state, which is indicative of the two-time scale behavior of the system, and is consistent with our observation that such process networks are modeled by systems of ODEs that are in a *nonstandard* singularly perturbed form.

Figure 6 shows the evolution of the total inert holdup for the same simulation run; note that this variable exhibits dynamics only in the slow time scale, a fact consistent with its being a true slow variable.

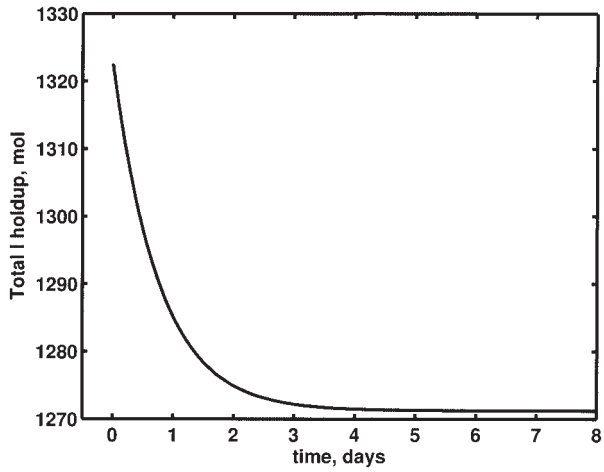

Figure 6. Evolution of the total inert holdup.

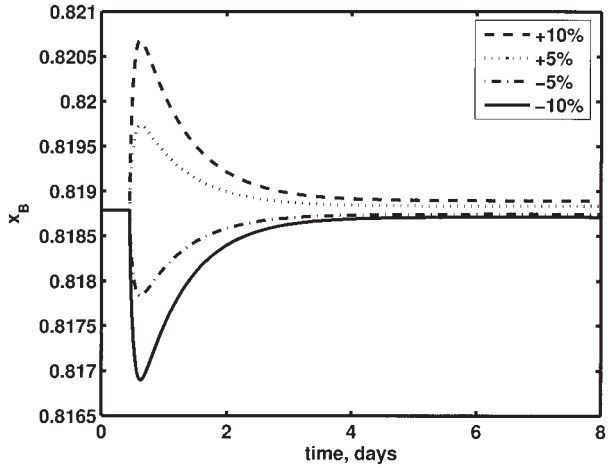

Figure 7. Response of the output x_B to changes in the recycle flow rate R.

According to the analysis results introduced above, the control of the product purity should be addressed in the fast time scale. After implementing the controllers (Eq. 26), using F and L as manipulated inputs, the remaining available manipulated input for the control of x_B is the recycle flow rate R.

Figures 7 and 8 illustrate the evolution of the product purity for different step changes in the recycle flow rate R, in the "open-loop" system mentioned above, indicating a fairly nonlinear dynamic response. Moreover, a plot of x_B vs. R at steady-state features an input multiplicity (Figure 9) that limits the applicability of linear controllers.[15] Consequently, we used the model of the fast dynamics of the network in Eq. 22 to design a nonlinear input–output linearizing output feedback controller with integral action[15] for x_B, requesting a critically damped second-order response:

$$x_B + \beta_{B,1}\frac{dx_B}{dt} + \beta_{B,2}\frac{d^2x_B}{dt^2} = x_{B,sp} \tag{34}$$

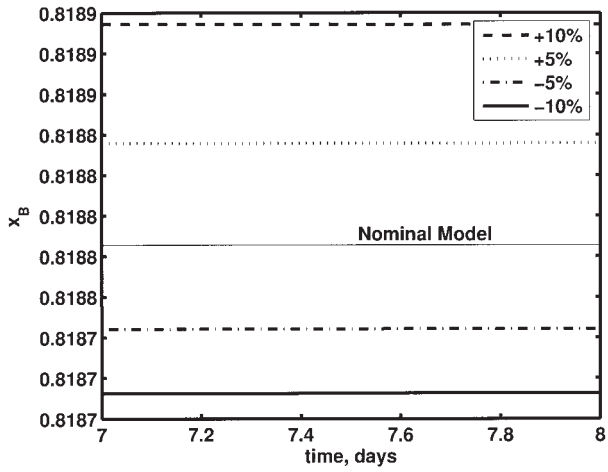

Figure 8. Detailed view of Figure 7.

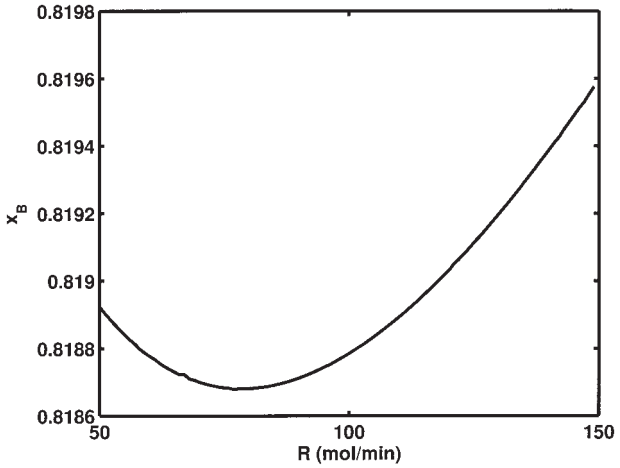

Figure 9. Input multiplicity of product purity loop.

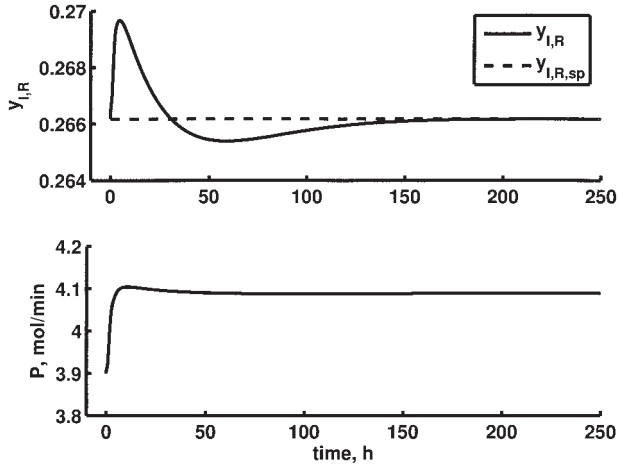

Figure 11. Closed-loop response for an unmeasured increase in $y_{I,o}$.

where $\beta_{B,1} = 40$ min and $\beta_{B,2} = 400$ min^2.

At first glance, a single controller, on the R–x_B loop, appears sufficient for addressing the main control objective. However, simulation results indicate that, to maintain x_B at the desired level when the network is subjected to a small (5%) increase in the mole fraction $y_{I,o}$, the recycle flow rate R would need to be increased to 505.8 mol/min (a fivefold increase from the nominal value). Thus, due to the inhibitive contribution of I in the reaction rate expression and, consequently, to the detrimental effect that its accumulation exerts on the operation of the network, the control of the impurity levels in the reactor is of critical importance and directly linked to the main objective of product purity control. According to our analysis, the control of $y_{I,R}$ should be addressed in the slow time scale using the purge stream as a manipulated input.

Motivated by the above, we used the coordinate transformation of Eq. 18 with $\phi(\mathbf{x}) = y_{I,R}$, along with the quasi-steady-state constraints stemming from setting the terms in Eq. 24 equal to zero, to obtain a description of the evolution of the reactor impurity mole fraction in the slow time scale. Subsequently, we used this description as the basis for synthesizing a nonlinear input–output linearizing controller that manipulates the purge flow rate to induce the following first-order response for $y_{I,R}$:

$$y_{I,R} + \beta_Y \frac{dy_{I,R}}{dt} = v \tag{35}$$

where $\beta_Y = 1000$ min and integral action is imposed on the $v - y_{I,R}$ dynamics.

Figures 10 and 11 show the closed-loop response of the reactor–condenser network in the case of an unmeasured increase in the inlet mole fraction of the inert $y_{I,o}$, from $y_{I,o} = 0.02$ to $y_{I,o} = 0.025$. The closed-loop behavior in the presence of the same disturbance, but considering, additionally, a 20% modeling error in the mass transfer coefficient of the product, $\mathcal{H}_B$, is presented in Figures 12 and 13. The proposed nonlinear control structure exhibits excellent performance in the presence of unmeasured disturbances, even when model mismatch is considered. The disturbance is rejected with small changes in the recycle rate and minimal effect on the product purity.

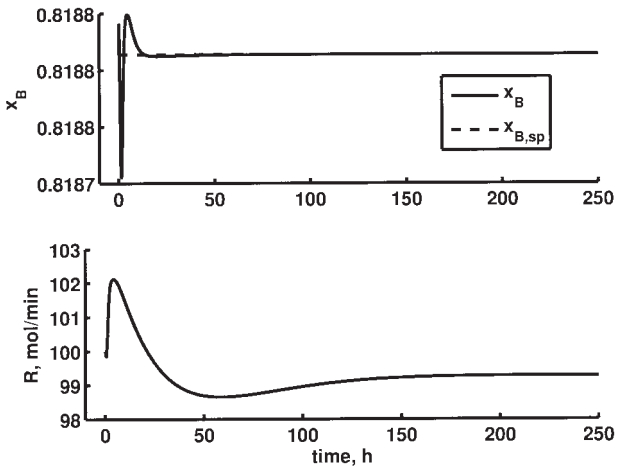

Figure 10. Closed-loop response for an unmeasured increase in $y_{I,o}$, from $y_{I,o} = 0.02$ to $y_{I,o} = 0.025$.

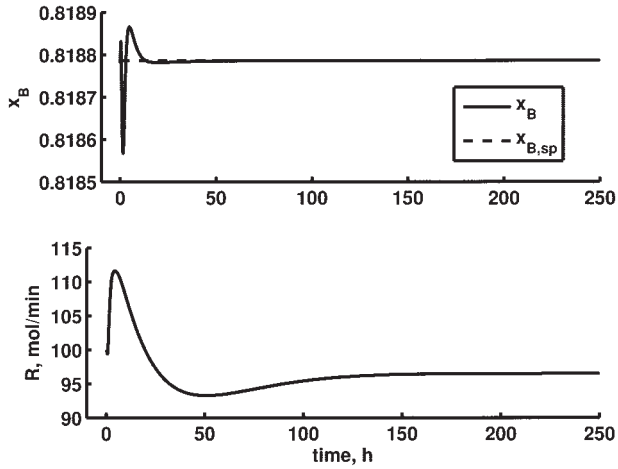

Figure 12. Closed-loop response for an unmeasured increase in $y_{I,o}$, from $y_{I,o} = 0.02$ to $y_{I,o} = 0.025$, in the presence of modeling errors.

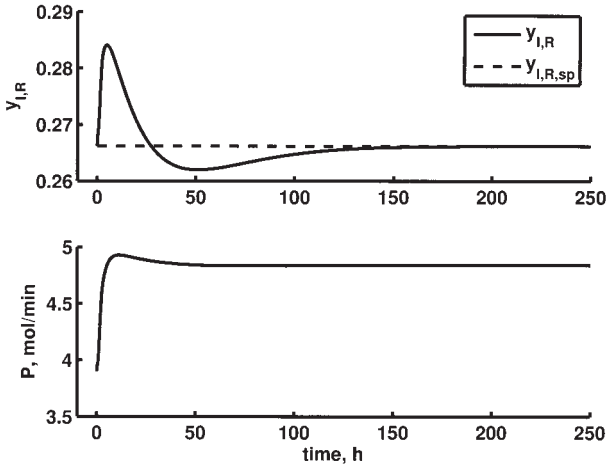

Figure 13. Closed-loop response for an unmeasured increase in $y_{I,o}$, in the presence of modeling errors.

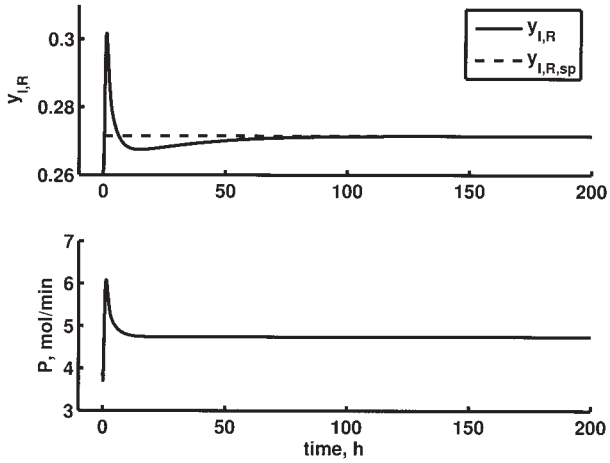

Figure 15. Closed-loop response for a 10% increase in F_o.

Figures 14–16 present the closed-loop response for a 10% increase in the network throughput (imposed by changing the feed flow rate F_o), along with a requested 2% increase in the inert mole fraction setpoint; this change in setpoint is necessary to prevent the purge flow rate from becoming too large, which would lead to an accrued loss of valuable raw material. In this case, too, the proposed nonlinear control structure exhibits very good performance and tracking ability, showing small changes in the product purity and imposing the desired inert mole fraction change.

Conclusions

In this work, we have shown that the presence of a small purge stream, used for the removal of small quantities of an impurity that is either present in the feed of a process network with recycle, or results as a reaction byproduct, causes the network to exhibit a two-time scale behavior. Specifically, the dynamics of such networks exhibit a fast dynamics, associated with the individual units, and a slow dynamics, that arises from the presence of small quantities of inert component in the feed, and of the purge stream with small flow rate. Within the framework of singular perturbations, we proposed a method for the derivation of reduced-order, nonstiff models for the behavior of such networks in each time scale. In addition to the generic network used for theoretical analysis, three prototype networks with recycle and purge streams were considered, and the slow dynamics of the networks was shown to be one-dimensional and directly associated with the total impurity holdup.

The proposed analysis also allowed for a rational separation of the available flow rates into two distinct sets of manipulated inputs, which act upon and can be used to address control objectives in the two time scales.

Finally, we provided a numerical example illustrative of the theoretical concepts developed in the article. In the example, a low-dimensional model of the slow dynamics was used in the synthesis of an input–output linearizing controller with integral action for the inert mole fraction in the reactor of the reactor–condenser process network. The proposed nonlinear controller

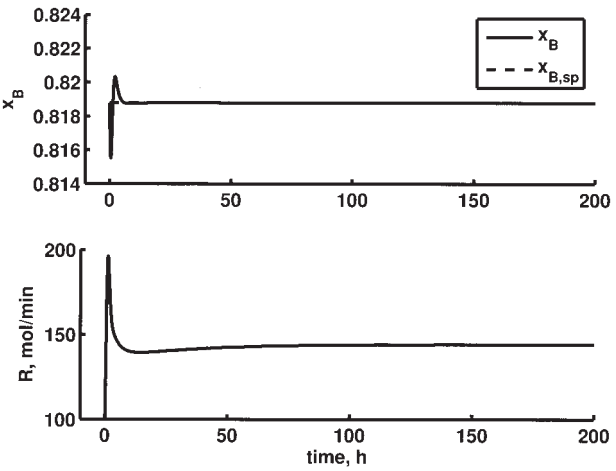

Figure 14. Closed-loop response for a 10% increase in F_o.

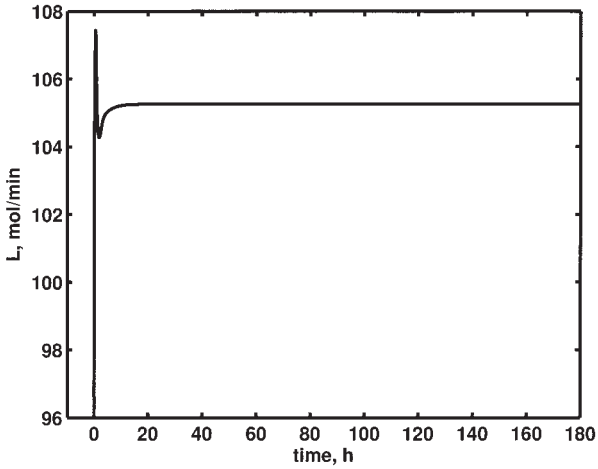

Figure 16. Closed-loop response of the product flow rate L for a 10% increase in F_o.

was tested by numerical simulation, indicating excellent set-point tracking performance and robustness.

Acknowledgments

A preliminary version of these results was presented at the ADCHEM'03 Conference, Hong Kong, January 2004.

Partial financial support for this work by the American Chemical Society Petroleum Research Fund (ACS-PRF Grant 38114-AC9) and National Science Foundation Chemical and Transport Systems (NSFCTS Grant 0234440) is gratefully acknowledged.

Literature Cited

1. Pushpavanam S, Kienle A. Nonlinear behavior of an ideal reactor separator network with mass recycle. *Chem Eng Sci.* 2001;57:2837-2849.
2. Kiss AA, Bildea CS, Dimian AC, Iedema PD. Design of recycle systems with parallel and consecutive reactions by nonlinear analysis. *Ind Eng Chem Res.* 2005;44:576-587.
3. Marquardt W. Fundamental modeling and model reduction for optimization based control of transient processes. Preprints of Chemical Process Control 6 (CPC-6), Tucson, AZ; 2000:30-60.
4. Yi CK, Luyben WL. Design and control of coupled reactor/column systems—Parts 1–3. *Comput Chem Eng.* 1997;21:25-68.
5. Chen YH, Yu CC. Design and control of heat integrated reactors. *Ind Eng Chem Res.* 2003;42:2791-2808.
6. Skogestad S. Control structure design for complete chemical plants. *Comput Chem Eng.* 2004;28:219-234.
7. Hangos KM, Alonso AA, Perkins JD, Ydstie BE. Thermodynamic approach to the structural stability of process plants. *AIChE J.* 1999; 45:802-816.
8. Ydstie BE. Passivity based control via the second law. *Comput Chem Eng.* 2002;26:1037-1048.
9. Kumar A, Daoutidis P. Dynamics and control of process networks with recycle. *J Process Contr.* 2002;12:475-484.
10. Belanger PW, Luyben WL. Plantwide design and control of processes with inerts. 1. Light inerts. *Ind Eng Chem Res.* 1998;37:516-527.
11. Luyben WL. Design and control of gas-phase reactor/recycle processes with reversible exothermic reactions. *Ind Eng Chem Res.* 2000; 39:1529-1538.
12. Dimian AC, Groenendijk AJ, Iedema PD. Recycle interaction effects on the control of impurities in a complex plant. *Ind Eng Chem Res.* 2001;40:5784-5794.
13. Contou-Carrère MN, Baldea M, Daoutidis P. Dynamic precompensation and output feedback control of integrated process networks. *Ind Eng Chem Res.* 2004;43:3528-3538.
14. Kumar A, Daoutidis P. Control of nonlinear differential equation systems. *Research Notes in Mathematics Series* (No. 397). New York, NY: Chapman & Hall/CRC; 1999.
15. Daoutidis P, Kravaris C. Dynamic output feedback control of minimum-phase nonlinear processes. *Chem Eng Sci.* 1992;47:837.

Manuscript received Apr. 11, 2005, and revision received Nov. 14, 2005.